

Effective and asymptotic scaling in a one-dimensional billiard problem

T. Holovatch ^{1,2}, Yu. Kozitsky ³, K. Pilorz ³, Yu. Holovatch ^{1,2,4,5}

¹ Institute for Condensed Matter Physics of the National Academy of Sciences of Ukraine, 79011 Lviv, Ukraine

² ⁴ Collaboration and Doctoral College for the Statistical Physics of Complex Systems, Lviv-Leipzig-Lorraine-Coventry, Europe

³ Institute of Mathematics, Maria Curie-Skłodowska University, 20-031 Lublin, Poland

⁴ Centre for Fluid and Complex Systems, Coventry University, Coventry CV1 5FB, UK

⁵ Complexity Science Hub Vienna, 1030 Vienna, Austria

Received March 26, 2025

The emergence of power laws that govern the large-time dynamics of a one-dimensional billiard of N point particles is analysed. In the initial state, the resting particles are placed in the positive half-line $x \geq 0$ at equal distances. Their masses alternate between two distinct values. The dynamics is initialized by giving the leftmost particle a positive velocity. Due to elastic inter-particle collisions, the whole system gradually comes into motion, filling both right-hand and left-hand half-lines. As shown by [Chakraborti S., Dhar A., Krapivsky P., SciPost Phys., 2022, **13**, 074], an inherent feature of such a billiard is the emergence of two different modes: the shock wave that propagates in $x \geq 0$ and the splash region in $x < 0$. Moreover, the behaviour of the relevant observables is characterized by universal asymptotic power-law dependencies. In view of the finite size of the system and of finite observation times, these dependencies only start to acquire a universal character. To analyse them, we set up molecular dynamics simulations using the concept of effective scaling exponents, familiar in the theory of continuous phase transitions. We present results for the effective exponents that govern the large-time behaviour of the shock-wave front, the number of collisions, the energies and momentum of different modes and analyse their tendency to approach corresponding universal values.

Key words: *billiards, one-dimensional cold gas, shock wave, scaling, scaling exponents, molecular dynamics*

To the 100th anniversary of Professor Ihor Yukhnovskii

In the year of centenary of the outstanding Ukrainian public and political figure Ihor Yukhnovskii (September 1, 1925 – March 26, 2024), the scientific community also celebrates him as the founder of Lviv school of statistical physics. Two of the authors of this article (Yu.K. and Yu.H.) had the honor of being among Prof. Yukhnovskii's direct students and working with him in the field of phase transition theory. His major contributions in this area include the pioneering work on the non-perturbative approach to the analysis of critical behaviour at continuous phase transitions, as summarized later in one of his monographs [1]. The topic we discuss in this article — the behaviour of a one-dimensional multi-particle billiard — may at first glance seem to be far removed from the problem of phase transitions. What is common, however, is the phenomenon of scaling — the emergence of universal power-law asymptotics — that govern the behaviour of different observables in both the continuous phase transition problem and in the billiards problem. This is what led us to the choice of this topic. After all, a deeper analysis of such an analogy may allow one to use methods and even concepts that are already well established in the study of one set of phenomena for the study of other problems. This is exactly the task we set in this work.

The further structure of the article is as follows. In the next section 1 we describe the phenomenon we are interested in and the observables in terms of which it is customary to describe this phenomenon. In

particular, we discuss the behaviour of a system of N elastically interacting particles after one of them is given a certain velocity at an initial time t , the N -particle billiard problem. Theoretical analysis suggests that for a large number of particles in such a system, a large-time power-law asymptotics of various observables is established. The scaling exponents that govern this asymptotics are universal: they are solely defined by space dimension and billiard symmetry. However, for a realistic case of finite N and t , the effective exponents might not yet reach their asymptotic values. This observation evokes a natural analogy with effective critical exponents, which describe the power-law behaviour of the thermodynamic or structural characteristics of a system undergoing a continuous phase transition. Such exponents are introduced into phase transition theory when analysing finite-size systems or when describing critical behaviour beyond a transition point. Their introduction is discussed in section 2. In order to track an emergence of the universal scaling laws, we set up the molecular dynamics simulations for a version of a one-dimensional billiard, as described in section 3. We end with conclusions and outlook in section 4.

1. One-dimensional many-particle billiards: phenomenon and its characteristics

In this paper, we consider the behaviour of the so-called multi-particle billiards. Mathematically, billiards describe the motion of mass points with elastic reflections [2, 3]. Billiards is not a single mathematical theory, this is rather a field to elaborate or test various methods, both analytical and numerical. Usually billiards are studied in the framework of dynamical systems theory and concern the behaviour of a single particle in a domain with elastic reflections from the boundary. A celebrated example is given by the Sinai billiard, as an illustration for interacting Hamiltonian system that displays physical thermodynamical properties [2]. One of the reasons for considering the problem of multi-particle billiards is that in this case they can serve as an intermediate bridge to explain the processes in a continuous medium based on elementary acts of inter-particle interaction via rigorous deviation of continuous hydrodynamics description starting from the atomistic one. This ambitious task is also known as Hilbert's 6th problem, suggested by David Hilbert in 1900 as "... the problem of developing mathematically the limiting processes ... which lead from the atomistic view to the laws of motion of continua. . .", see, e.g., [4] for more discussion.

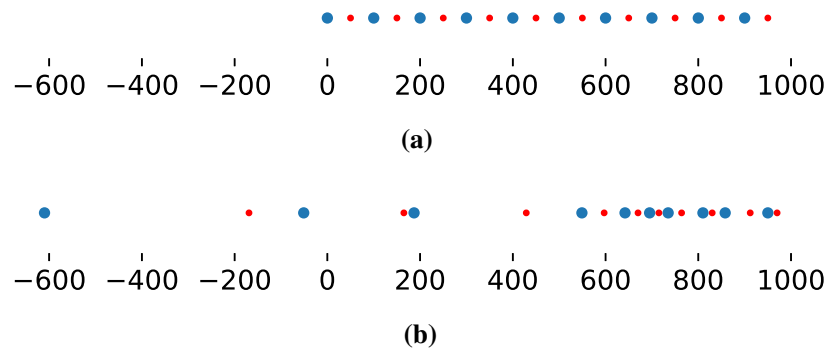


Figure 1. (Colour online) The phenomenon we are interested in this article. N point-like particles of possibly different masses are at rest and form a one-dimensional chain, that fills in the half-space $x \geq 0$, panel (a). The first particle acquires certain initial velocity, starts moving to the right and, thus, due to elastic collisions, the whole system gradually comes into motion, filling both right-hand and left-hand subspaces, panel (b). An inherent feature of the dynamics of such a billiard is the emergence of two different modes [5]: the shock wave that propagates in the right-hand side $x \geq 0$ and the splash region formed by the particles that move with negative velocities in the left-hand side $x < 0$. In our analysis we consider particles of two masses M and m (blue and red balls) assuming that they alternate and are equidistantly located at the initial moment of time.

We focus on the behaviour of one-dimensional billiards. In particular, we consider the set of N

point-like particles, as depicted in figure 1. In the initial state, all particles — ‘billiard balls’ — are at rest in the half-space $x \geq 0$ and are fixed at certain locations, figure 1a. Then, the first ball acquires an initial velocity v_0 directed to the right in the figure. It undergoes an elastic collision with the second ball, then the next collision occurs, and gradually, under the influence of elastic inter-ball collisions, that conserve momentum and energy, the whole system begins to move, figure 1b. We are interested in the asymptotic behaviour of such a billiard, which arises in the limit of a large number of balls and large observation times.

One immediately notes that the problem is trivial when all the particles are of the same mass. Indeed, since the collisions are elastic, after the first particle is set in motion, a domino effect is observed: the first particle takes the place of the second one and stops, the second particle takes the place of the third, and so on. This degeneracy is removed when particle masses are different. In our analysis we consider particles of two masses M and m assuming that they alternate, as shown by blue and red balls in figure 1. Such a system of alternating particles is known as an alternating hard particle gas. It is widely used for analysis of heat transport and hydrodynamics in one dimension [6–8], for the recent studies see [5, 9] and references therein.

We should also note the intrinsic symmetry of this problem: while at the initial moment of time, the right-hand half-space $x \geq 0$ is filled with particles, the left-hand half-space $x < 0$ is empty. This distinguishes it from a similar problem where particles fill the entire space and the dynamics is initiated by letting to move the particle at the origin. This latter case was considered in reference [10], where it was shown that the system large-time dynamics is governed by power laws. In particular, for the d -dimensional billiard, the number of collisions $C(t)$ and the number of moving particles $N(t)$ were found to scale as $C(t) \sim t^\eta$, $N(t) \sim t^\xi$ with $\eta = 2(d+1)/(d+2)$, $\xi = 2d/(d+2)$, leading to $\eta = 2\xi = 4/3$ for $d = 1$. Moreover, noticing that the release of energy, when the initial particle comes to motion, makes the phenomenon similar to the explosion in a continuous medium, it is argued that the above scaling laws coincide with those that describe the shock wave emanating from an explosion in the hydrodynamic theory [11]. In turn, it leads to the power-law asymptotics for the shock-wave front $\mathcal{R}(t) \sim t^\delta$, with $\delta = 2/(d+2)$. The above-mentioned symmetry restriction of the billiard of figure 1 leads to a number of unusual surprising phenomena. A detailed analysis of the dynamics of such a billiard showed [5] that its asymptotic behaviour is characterized by two regimes: the shock wave that propagates in the right-hand side $x \geq 0$ and the splash region formed in the left-hand side $x < 0$ by the particles that move with negative velocities. The shock-wave front is described by the hydrodynamic equations, although differing from those of the symmetric case [10, 12, 13]. Notably, the particles in the splash region $x < 0$ after experiencing a period of collisions move ballistically and their movement is non-hydrodynamic.

Let us quote some of the asymptotic laws that govern the dynamics of the one-dimensional splash problem as they were derived in reference [5]:

- With the span of time, all energy is accumulated in the splash region $x < 0$. Energy of particles in the right-hand half-space decays as

$$\mathcal{E}_{x \geq 0}(t) \sim t^{-\beta}. \quad (1)$$

- The shock-wave front (i.e., the coordinate of the front-right moving particle) propagates sub-ballistically with the exponent $\delta < 1$:

$$\mathcal{R}(t) \sim t^\delta. \quad (2)$$

- The number of the inter-particle collisions grows as

$$C(t) \sim t^\eta. \quad (3)$$

- The growth of total momenta of particles in the left-hand and in the right-hand half-spaces, $\mathcal{P}_{x < 0}(t)$ and $\mathcal{P}_{x \geq 0}(t)$ is governed by the same exponent:

$$-\mathcal{P}_{x < 0}(t) \sim \mathcal{P}_{x \geq 0}(t) \sim t^\gamma. \quad (4)$$

Obviously, the sum $\mathcal{P}_{x \geq 0}(t) + \mathcal{P}_{x < 0}(t)$ is constant and due to the momentum conservation law it equals the momentum of the incipient moving particle.

Table 1. Asymptotic values of the exponents governing the scaling laws (1)–(4) for the one-dimensional splash problem [5].

β	δ	η	γ
0.11614383675	0.6279520544	1.255904109	0.2559041088

Along with these asymptotic laws, the relations between the exponents governing the power-law behaviour equations (1)–(4) were derived:

$$\delta = \frac{2 - \beta}{3}, \quad \eta = 2\delta, \quad \gamma = \frac{1 - 2\beta}{3}, \quad (5)$$

and the values of the exponents were obtained [5]. The latter are displayed in table 1. Needless to emphasize the striking similarity of the relations (5) with the familiar scaling relations arising in the theory of critical phenomena [14–16].

Strictly speaking, universal power-law asymptotics, equations (1)–(4) with the exponent values given in table 1 are observed in the limit of an infinite number of particles (or in the hydrodynamic limit of a continuous medium). It is natural to expect (as we will see below this is indeed the case) that the laws are violated for finite observation times and system sizes. Again, the situation is similar to the scaling laws governing the critical behaviour at continuous phase transitions. There, the universal asymptotics is inherent only in the thermodynamic limit and at the transition point, otherwise non-universal exponents are observed. In order to use this analogy further, in the next section we show how the asymptotic (universal) and the effective (system-specific) critical exponents are introduced in the phase transition description.

2. Asymptotic and effective exponents in the continuous phase transition description

The concept of a critical exponent is one of the central concepts in the theory of continuous phase transitions. Critical exponents describe the singular power-law behaviour at a phase transition. They are universal (common to a wide class of different systems) and are the subject of a detailed analysis in the experiment, in theory, and in computer simulations [14–16]. Strictly speaking, the asymptotic critical exponents are universal, which are determined directly at the phase transition point. For definiteness, let us take a thermodynamic phase transition as an example, when the controlling parameter is temperature T , and the other parameters, such as the external field, have already acquired their critical values. Then, the *asymptotic critical exponent* ν for the observable $O(\tau)$ is defined as the limit:

$$\nu = - \lim_{\tau \rightarrow 0} \frac{\ln O(\tau)}{\ln \tau}, \quad (6)$$

where $\tau = |T - T_c|/T_c$ is the dimensionless temperature measuring the distance to the critical point T_c . Formula (6) means that the leading singularity for $O(\tau)$ is of the power-law form:

$$O(\tau) \sim \tau^{-\nu} (1 + \dots), \quad \tau \rightarrow 0, \quad (7)$$

and the dots denote the sub-leading terms.

As mentioned above, the asymptotic critical exponents (6), (7) are universal. They depend only on such global factors as space dimension, inter-particle interaction range, system symmetry. However, in practice, both in experiments and in computer simulations, one has to deal with non-universal critical exponents, which depend on the system details. These are commonly called *effective critical exponents*. At least two reasons for the appearance of such an effective critical behaviour can be pointed out. These are: (i) measurements outside the critical point T_c (i.e., at $\tau \neq 0$) and (ii) simulations of finite-size systems. Indeed, in an experiment, whether computer or real, it is not the singularity itself that is observed, but

only the tendency for its appearance. To be more specific concerning these reasons, herein below we refer to the usual ways the effective exponents are introduced:

- (i) To describe the critical behaviour when the asymptotic scaling (7) is not yet reached, it is convenient to define the effective critical exponents via [17, 18]:

$$\nu_{\text{eff}}(\tau) = -\frac{d \ln O(\tau)}{d \ln \tau}. \quad (8)$$

Obviously, the effective exponents coincide with the asymptotic ones in the limit $\tau \rightarrow 0$.

- (ii) To study the emergence of power-law singularities by computer simulations with a finite number of particles N , the ideas of finite-size scaling, FSS, apply [19, 20]. They are based on the fact that when approaching $\tau = 0$, the correlation length ξ becomes the only characteristic scale of the system. At $\tau = 0$, the correlation length diverges with the critical exponent ν , $\xi \sim \tau^{-\nu}$. In turn, inverting this dependence as $\tau \sim \xi^{-1/\nu}$, enables one to represent the power-law asymptotic (7) as a dependence of the observable on the correlation length: $O \sim \xi^{\nu/\nu}$. Assuming that the maximal correlation length increases linearly with the system size L , one arrives¹ at the FSS relation, determining the leading power-law singularity as:

$$O(L) \sim L^{\nu/\nu}(1 + \dots), \quad L \rightarrow \infty, \quad (9)$$

and, as in equation (8) the dots denote the sub-leading terms. Since computer simulations are carried out for finite L , in practice the effective exponents are determined:

$$\frac{\nu}{\nu}|_{\text{eff}}(L) = \frac{d \ln O(L)}{d \ln L}. \quad (10)$$

It is worth noting that reasons (i) and (ii) are also related by the fact that the correlation length ξ cannot be infinite for a finite-size system. The same applies to an infinite system beyond the critical point $\tau = 0$.

Effective critical exponents and their evolution to the asymptotic values are the subject of detailed studies, see, for example, [21–23] or recent papers [24, 25] for more references. In the mentioned papers, effective critical exponents describe continuous phase transitions in various magnetic, structurally disordered, or fluid systems. In the next section, we apply this concept to the analysis of power-law scaling in the one-dimensional billiard splash problem.

3. Molecular dynamic simulations of a one-dimensional N -particle billiard

In this section, we present the results of computer simulations of the one-dimensional N -particle billiard shown in figure 1. Note that, unlike the simulations of one-dimensional billiards in references [5, 10, 12, 13], where the initial coordinates of particles were considered as random, in our case at time $t = 0$, the particles are located at equal distances, as shown in figure 1a. Thus, there is no need to perform the averaging over different starting configurations of particle locations. We performed the molecular dynamics (MD) simulations, solving the equations of motion for a system of $N = 10\,000$ particles. We took the particles to be of two different masses, M and m (blue and red balls in figure 1), assuming that they are point-like and are placed at equal distances r_0 at the initial moment of time $t = 0$. We consider that the incipient particle is of a larger mass $M > m$ and it acquires, at $t = 0$, the initial velocity v_0 directed to the right. Since all particles subsequently interact through elastic collisions, the total momentum and total energy of all particles are conserved throughout the entire evolution of the system and are equal to the initial energy and momentum of the incipient particle, $E_0 = Mv_0^2/2$ and $P_0 = Mv_0$, correspondingly. Note that the evolution of the billiard in which the first particle is of lighter mass m is analogous. Indeed, after

¹This assumption holds only below the so-called upper critical dimension d_{uc} . For $d > d_{\text{uc}}$, the correlation-length scaling is governed by the critical exponent φ (koppa): $\xi \sim L^\varphi$, $\varphi = d/d_{\text{uc}}$. However, this discussion goes beyond the scope of this paper [16].

a collision with the second heavier particle, the first particle acquires a negative velocity and continues its collisionless² leftward motion at a constant velocity. Instead, the subsequent dynamics of the system is initiated by the heavier particle of mass M , which moves rightward, as in the previous case.

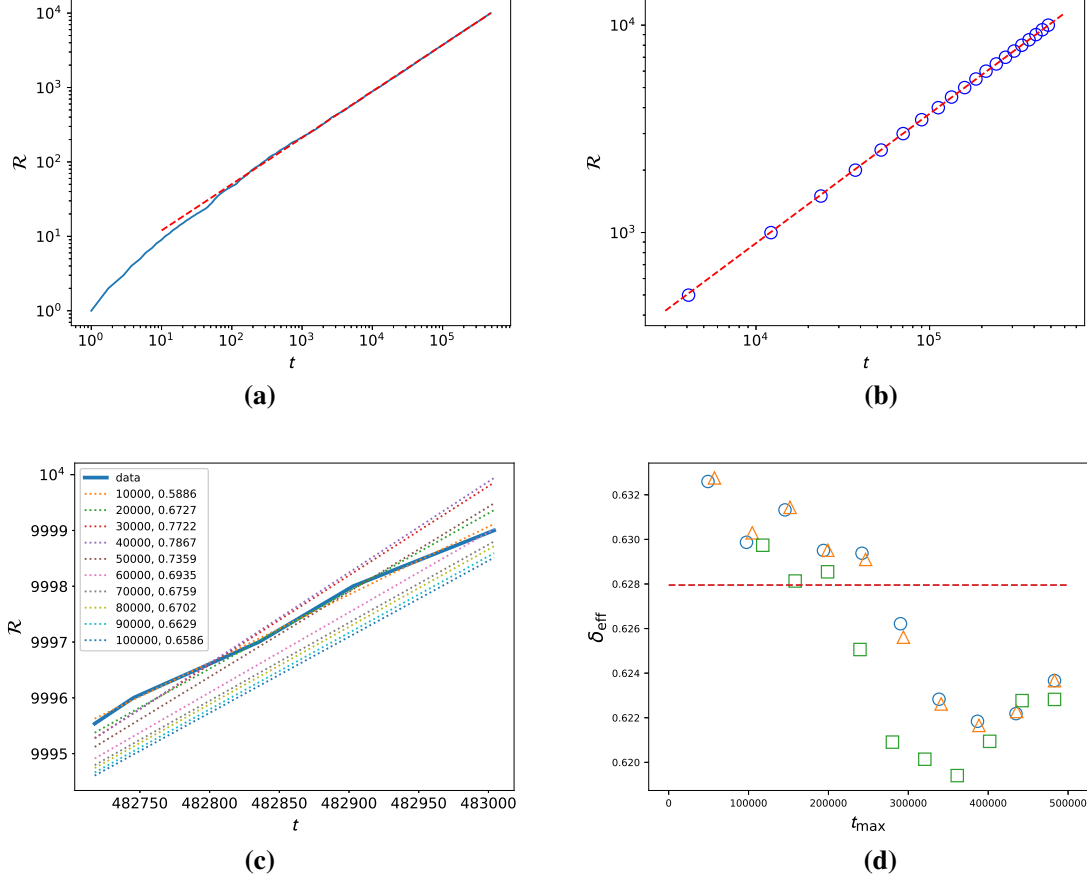


Figure 2. (Colour online) Shock-wave front position $\mathcal{R}(t)$ for the one-dimensional billiard of particles of two alternating masses, $M/m = 2$, that are equidistantly located at the initial moment of time, blue and red balls in figure 1. **(a):** Data points (seen as a blue solid curve) and their fit by the power-law dependency $\mathcal{R}(t) \sim t^\delta$ (red dashed line). **(b):** Data points (blue circles) correspond to the time instances when the shock wave passes each $500 \times k$ th particle, $k = 1, \dots, 20$. Red dashed line is a guideline for the eye and shows a power-law dependency with the asymptotic exponent $\delta = 0.62795$, see table 1. **(c):** Data points (seen as a blue solid curve) correspond to the time interval when the last 10^4 collisions took place. The dashed lines describe the fitted power-law dependencies taking into account the last $n = 10^4 \times k$ collisions, $k = 1, \dots, 10$. The legend displays n together with the exponent δ_{eff} as it results from the fit for each n . **(d):** Effective exponent δ_{eff} obtained as a result of a power-law fit for $\mathcal{R}(t)$ in the region $[t_{\min}, t_{\max}]$ with $t_{\min} = 10^3, 10^4, t_{10\%}$, shown by circles, triangles, and squares, correspondingly, and $t_{10\%} = 117\,753$ is the time when 10% of all collisions have occurred. In each case, the maximal value of t_{\max} is limited by the time when the shock wave reaches the rightmost particle $t_{\max} = t_{\text{final}} = 483\,004$.

We are interested in the time evolution of the shock-wave front $\mathcal{R}(t)$, the total energy of particles in the region $x \geq 0$, $\mathcal{E}_{x \geq 0}(t)$, the number of collisions $\mathcal{C}(t)$, and the total momenta of particles in the splash region $x < 0$, $\mathcal{P}_{x < 0}(t)$. In particular, our goal is to check whether their time dynamics are characterized by power-law asymptotics (1)–(4) with the exponents given in table 1. In what follows, we present the results in dimensionless variables, measuring distance, energy, momentum, and time in units of r_0 , E_0 , P_0 , and $t_0 = r_0/v_0$, respectively. Since we are dealing with a finite number of particles,

²Although this statement sounds reasonable, it has been proven only under certain conditions and still remains as a conjecture [5].

the observation time is limited by time t_{final} , when the last of $N = 10\,000$ particles is set in motion. For the parameters chosen in our simulations ($E_0 = 1$, $M/m = 2$), the last, rightmost, particle starts moving after the system experiences $C_{\text{final}} = 13\,369\,302$ collisions. This corresponds to $t_{\text{final}} = 483\,004$ in the dimensionless variables. Accordingly, all further results concern the time window between $t = 0$ and $t = t_{\text{final}} = 483\,004$.

Blue curve in figure 2a shows the time evolution of the shock-wave front position (coordinate of the rightmost moving particle) $\mathcal{R}(t)$. After rather short initialization period, $t \simeq 10^2 - 10^3$, the system tends to develop a power-law dependence $\mathcal{R}(t) \sim t^\delta$, as shown by the dashed red line in the double logarithmic plot in the figure. The latter is displayed more in detail in figure 2b, where the blue circles mark the coordinates of the shock-wave front as it reaches every 500th particle. The red dashed line in the figure shows the power-law dependence with the asymptotic value of the exponent δ taken from table 1. At first glance, such a coincidence of simulated and analytically predicted data can serve as a good confirmation that the asymptotic scaling is observed. However, the linear dependence depicted in this figure serves only as an eye-guide, since it is not obtained as a result of the simulation data fit. In fact, the situation is more complicated and typical of the analysis of finite-sized systems. Figure 2c shows the behaviour of the tail of $\mathcal{R}(t)$: its change in time is always discrete (blue curve) and the value of the power-law fit exponent δ_{eff} will depend on the time window within which such a fit is performed (dashed lines). The legend shows the values of the time windows together with the values of the effective exponents that correspond to the fits. It is obvious that the time windows chosen for the illustration in figure 2c are too small to judge about the asymptotics. However, the general problem remains: the time intervals, on the one hand, should correspond to large times (starting from some ‘equilibration’ time t_{min} when the system has experienced a comparatively large number of collisions) and, on the other hand, the time window should be large enough to smoothen the fluctuations, that are inevitably present even for large times. With these two caveats in mind, we approach finding the effective scaling exponent δ_{eff} as depicted in figure 2d. The exponent δ_{eff} shown in this figure corresponds to power-law fits for different time intervals $[t_{\text{min}}, t_{\text{max}}]$. We made three different choices for t_{min} : $t_{\text{min}} = 10^3$, 10^4 , $t_{10\%}$, shown by circles, triangles, and squares, correspondingly. Time $t_{10\%} = 117\,753$ is the time when 10% of all collisions have occurred. In turn, for each t_{min} , the value of t_{max} increased up to t_{final} , when the shock wave reached the rightmost particle. The dependence of $\delta_{\text{eff}}(t_{\text{max}})$ with an increase of t_{max} is shown in the figure. As one can see from the figure, with an increase of t_{max} , δ_{eff} tends to approach its asymptotic value shown by the red dashed line. This trend is maintained for all considered initial times t_{min} .

Based on the results of the shock-wave front $\mathcal{R}(t)$ analysis, we defined in a similar way the effective scaling exponents for the total energy of particles in the $x \geq 0$ region $\mathcal{E}_{x \geq 0}(t)$, the total number of collisions $C(t)$, and the total momentum of particles in the $x < 0$ region $\mathcal{P}_{x < 0}(t)$. The results are shown in figure 3. Similar to figure 2b, the plots in figures 3a, 3c, 3e exhibit power-law behaviour, which at first glance is well described by the asymptotic exponents in table 1. However, a more detailed analysis shows the scaling with varying effective exponents, as depicted in the plots of the right-hand column of figure 3. With an increasing observation time, all exponents show a tendency to approach their asymptotic values. However, the convergence is different. While the effective exponents δ_{eff} , β_{eff} , η_{eff} differ from their asymptotic counterparts within the third significant digit only, the exponent γ_{eff} for the total momentum of particles in the $x < 0$ region $\mathcal{P}_{x < 0}(t)$ remains further away, $\gamma_{\text{eff}} - \gamma \simeq 0.02$.

4. Conclusions and outlook

A characteristic feature of the billiard problem we have considered here is the lack of a priori randomness, neither in the distribution of masses nor in the inter-particle distances. Therefore, the emergence of the hydrodynamic power-law asymptotics — pointing to the stochastic background of the underlying process — may be interpreted as a kind of self-averaging in the system. As it follows from the simulations we have performed, the exponents that govern the scaling of different observables are system-dependent. In our case, such a dependence manifests itself as their change with the system size N and the size of the time window in which the fit is performed. To interpret such a behaviour, it is instructive to make use of the concept of effective critical exponents, as introduced in the theory of continuous phase transitions. The observed effective critical exponents, figures 2d, 3b), 3d), 3f), tend to

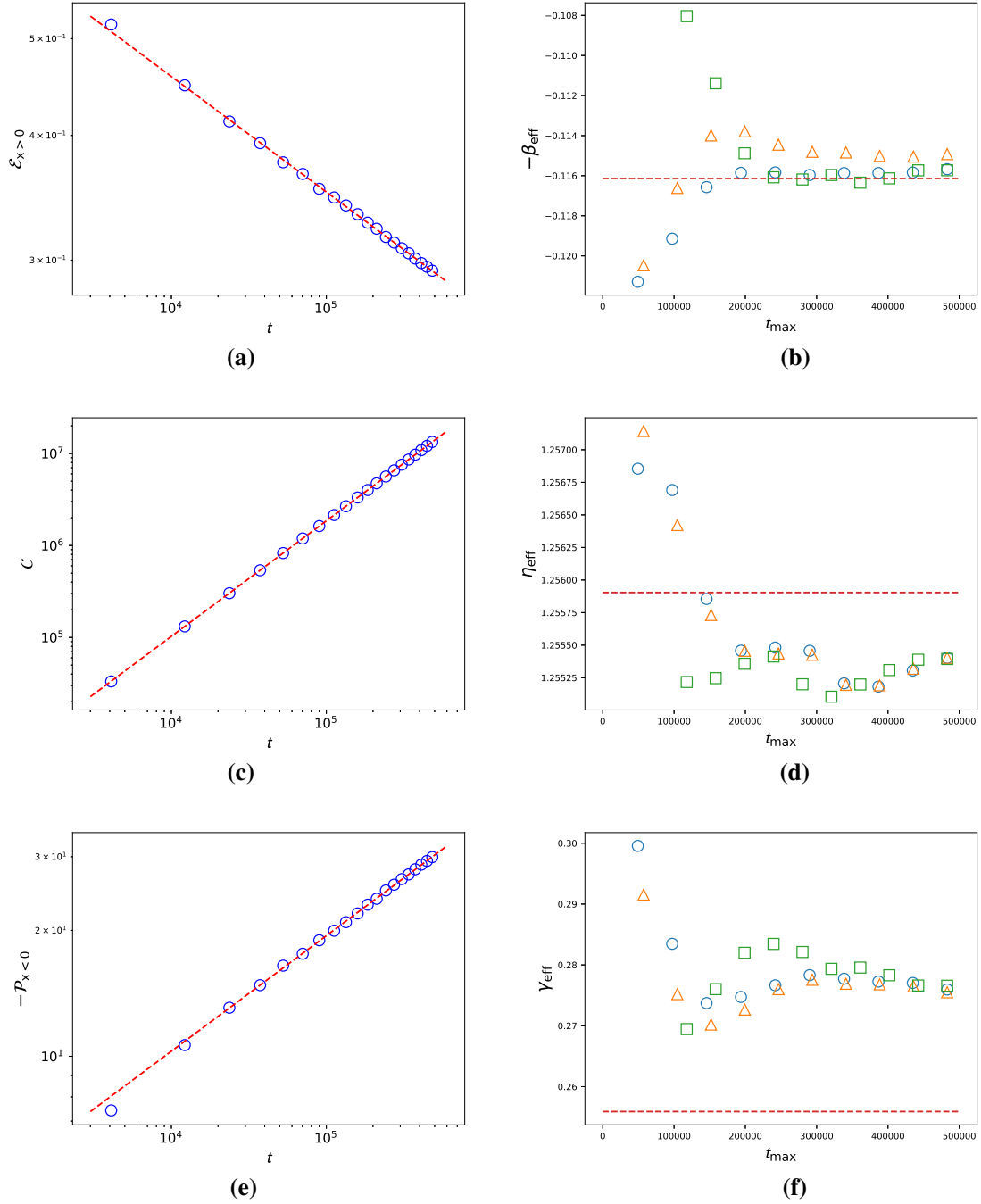


Figure 3. (Colour online) *Left panels* display time dependencies of (a): total energy of particles in the $x \geq 0$ region $\mathcal{E}_{x \geq 0}(t)$, (c): number of collisions $C(t)$, and (e): total momentum of particles in the $x < 0$ region $\mathcal{P}_{x < 0}(t)$. Data points (blue circles) correspond to time instances when the shock wave passes each $500 \times k$ th particle, $k = 1, \dots, 20$. Red dashed lines show power-law dependencies with the asymptotic exponents, as given in table 1. *Right panels* give the effective scaling exponents for the quantities displayed in the left panels. Similar as in figure 2d, the exponents were obtained as a result of power-law fits in the region $[t_{\min}, t_{\max}]$ with $t_{\min} = 10^3, 10^4, t_{10\%}$, shown by circles, triangles, and squares, correspondingly. See the text and the caption of figure 2d for more description. Red dashed lines show values of the asymptotic exponents given in Table 1.

change with the growth of N (therefore, with the growth of the time window too) and approach their asymptotic values displayed in table 1. As mentioned above, these values were obtained analytically by solving equations of a continuous medium. Therefore, this trend also serves as an indirect indication that the considered here discrete system of equidistantly distributed alternating hard particles reproduces the continuous medium in the limiting case.

Acknowledgement

We thank Pavel Krapivsky, whose talk at the Ising lectures in Lviv [26] motivated us to perform this study.

References

1. Yukhnovskii I. R., Phase Transitions of the Second Order. Collective Variables Method, World Scientific, Singapore, 1987, doi:10.1142/0289.
2. Sinai Y. G., Introduction to Ergodic Theory, Mathematical Notes, Vol. 18, Princeton University Press, Princeton, New Jersey, 1976.
3. Tabachnikov S., Geometry and Billiards, The Student Mathematical Library, Vol. 30, American Mathematical Society, Providence, Rhode Island, 2005, doi:10.1090/stml/030.
4. Gorban A. N., Philos. Trans. R. Soc. A, 2018, **376**, No. 2118, 20170238, doi:10.1098/rsta.2017.0238.
5. Chakraborti S., Dhar A., Krapivsky P. L., SciPost Phys., 2022, **13**, 074, doi:10.21468/SciPostPhys.13.3.074.
6. Garrido P. L., Hurtado P. I., Nadrowski B., Phys. Rev. Lett., 2001, **86**, 5486–5489, doi:10.1103/PhysRevLett.86.5486.
7. Dhar A., Phys. Rev. Lett., 2001, **86**, 3554–3557, doi:10.1103/PhysRevLett.86.3554.
8. Grassberger P., Nadler W., Yang L., Phys. Rev. Lett., 2002, **89**, 180601, doi:10.1103/PhysRevLett.89.180601.
9. Lepri S., Livi R., Politi A., Phys. Rev. Lett., 2020, **125**, 040604, doi:10.1103/PhysRevLett.125.040604.
10. Antal T., Krapivsky P. L., Redner S., Phys. Rev. E, 2008, **78**, 030301, doi:10.1103/PhysRevE.78.030301.
11. Landau L. D., Lifshitz E. M., Fluid Mechanics, Course of Theoretical Physics, Vol. 6, Elsevier, Amsterdam, Boston, Heidelberg, 1987.
12. Chakraborti S., Ganapa S., Krapivsky P. L., Dhar A., Phys. Rev. Lett., 2021, **126**, 244503, doi:10.1103/PhysRevLett.126.244503.
13. Ganapa S., Chakraborti S., Krapivsky P. L., Dhar A., Phys. Fluids, 2021, **33**, No. 8, 087113, doi:10.1063/5.0058152.
14. Fisher M. E., Rep. Prog. Phys., 1967, **30**, No. 2, 615, doi:10.1088/0034-4885/30/2/306.
15. Stanley H. E., Introduction to Phase Transitions and Critical Phenomena, International series of monographs on physics, Vol. 46, Oxford University Press, New York, Oxford, 1987.
16. Berche B., Ellis T., Holovatch Y., Kenna R., SciPost Phys. Lect. Notes, 2022, 60, doi:10.21468/SciPostPhysLectNotes.60.
17. Kouvel J. S., Fisher M. E., Phys. Rev., 1964, **136**, A1626–A1632, doi:10.1103/PhysRev.136.A1626.
18. Riedel E. K., Wegner F. J., Phys. Rev. B, 1974, **9**, 294–315, doi:10.1103/PhysRevB.9.294.
19. Privman V., In: Finite Size Scaling and Numerical Simulation of Statistical Systems, Privman V. (Ed.), World Scientific, Singapore, 1990, 1–98, doi:10.1142/9789814503419_0001.
20. Ardourel V., Bangu S., Stud. Hist. Philos. Sci., 2023, **100**, 99–106, doi:10.1016/j.shpsa.2023.05.010.
21. Folk R., Moser G., J. Phys. A: Math. Gen., 2006, **39**, No. 24, R207, doi:10.1088/0305-4470/39/24/R01.
22. Dudka M., Folk R., Holovatch Y., Ivaneiko D., J. Magn. Magn. Mater., 2003, **256**, No. 1, 243–251, doi:10.1016/S0304-8853(02)00569-3.
23. Perumal A., Srinivas V., Rao V. V., Dunlap R. A., Phys. Rev. Lett., 2003, **91**, 137202, doi:10.1103/PhysRevLett.91.137202.
24. Ruiz-Lorenzo J. J., Dudka M., Holovatch Y., Phys. Rev. E, 2022, **106**, 034123, doi:10.1103/PhysRevE.106.034123.
25. Ruiz-Lorenzo J. J., Dudka M., Krasnytska M., Holovatch Y., Phys. Rev. E, 2025, **111**, 024127, doi:10.1103/PhysRevE.111.024127.
26. Ising lectures, 2024, Annual Workshop on Critical Phenomena and Complex Systems, URL <https://icmp.lviv.ua/ising/archive/2024.html>.

Ефективний та асимптотичний скейлінг в одній задачі про одновимірний більярд

Т. Головач^{1,2}, Ю. Козицький³, К. Пілож³, Ю. Головач^{1,2,4,5}

¹ Інститут фізики конденсованих систем НАН України, 79011 Львів, Україна

² Співпраця \mathbb{L}^4 і Коледж докторантів "Статистична фізика складних систем", Ляйпціг-Лотарингія-Львів-Ковентрі, Європа

³ Інститут математики, Університет Марії Склодовської-Кюрі, Люблін, 20-031, Польща

⁴ Центр плинних і складних систем, Університет Ковентрі, Ковентрі, CV1 5FB, Велика Британія

⁵ Центр науки про складність, Відень, 1030, Австрія

Проаналізовано появу степеневих законів, які керують довгочасовою динамікою одновимірного більярду N точкових частинок. У початковому стані частинки розташовані в додатній півлінії $x \geq 0$ на однаковій відстані. Їхні маси чергуються між двома різними значеннями. Динаміка ініціалізується наданням крайній лівій частинці додатної швидкості. Завдяки пружним міжчастинковим зіткненням вся система поступово приходить в рух, заповнюючи як праву, так і ліву півлінії. Як показано в [Chakraborti S., Dhar A., Krapivsky P., SciPost Phys., 2022, **13**, 074], особливістю такого більярду є поява двох різних режимів: ударної хвилі що поширюється в $x \geq 0$ та області бризок в $x < 0$. Крім того, поведінка відповідних спостережуваних характеризується універсальними асимптотичними степеневими залежностями. З огляду на скінчений розмір системи і скінчений час спостереження ці залежності тільки починають набувати універсального характеру. Для їх аналізу ми проводимо симуляції методом молекулярної динаміки і використовуємо відому в теорії неперервних фазових переходів концепцію ефективних показників скейлінгу. Ми представляємо результати для ефективних показників, які керують довгочасовою поведінкою фронту ударної хвилі, кількості зіткнень, енергії та імпульсу різних мод та аналізуємо їх тенденцію наближатися до відповідних універсальних значень.

Ключові слова: більярд, одновимірний холодний газ, ударна хвиля, скейлінг, показники скейлінгу, молекулярна динаміка